DOI: 10.1021/ma902516m

Macromolecules
ARTICLE

Microphase Separation Induced by Complexation of Ionic−Non-Ionic Diblock Copolymers with Oppositely Charged Linear Chains

Anna S. Bodrova,[†] Elena Yu. Kramarenko,[†] and Igor I. Potemkin*[,†,‡]

[†]*Department of Physics, Moscow State University, Moscow 119992, Russian Federation, and* [‡]*Department of Polymer Science, University of Ulm, 89069 Ulm, Germany*

Received November 13, 2009; Revised Manuscript Received January 14, 2010

ABSTRACT: We develop a theory of microphase separation in a solution precipitate of flexible AB block copolymers consisting of charged (A) and neutral (B) blocks which are complexed with oppositely charged linear chains (C) via electrostatic interactions. We analyze regimes of selective solvents: the solvent is Θ for the A blocks and the C chains, whereas it is poor for the B blocks. Despite the selectivity, stoichiometric complexes precipitate because of fluctuations induced electrostatic attraction. Depending on composition of the diblock copolymer, selectivity of the solvent and fraction of charged groups, direct and inverse spherical, cylindrical and lamellar structures can be stable in the precipitant. Phase diagrams are constructed in the strong segregation approximation. Morphological transitions induced by changes of solvent quality and fraction of charged groups are predicted.

1. Introduction

Enhanced solubility of polyelectrolytes in dilute aqueous solutions is usually attributed to the existence of long-range electrostatic repulsion between charged groups on the chains and to the presence of mobile counterions.[1] That is why such systems are very sensitive to variation of pH, salt concentration and temperature. For example, adding low-molecular-weight salt diminishes solubility of polyelectrolytes.[2] The presence of amphiphilicity in the primary structure of charged macromolecules, i.e., the existence of soluble and insoluble groups, enriches behavior of the solutions. For example, diblock copolymers comprising soluble ionic (hydrophilic) and insoluble nonionic (hydrophobic) blocks form micelles in dilute aqueous solutions.[3−8] Dense core of the micelles is formed by insoluble blocks, and swollen polyelectrolyte blocks in the corona provide stability (solubility) of the micelles. The form of the micelles is primarily controlled by chemical composition of the copolymer. Spherical micelles are stable if the soluble block is long enough.[4,7] Otherwise, cylindrical micelles and vesicles (closed bilayers) are formed (the so-called crew-cut regime).[4,7] One of perspective applications of the micelles is to use them as nanocontainers for delivery of either hydrophobic species incorporated in the cores or oppositely charged molecules forming stable interpolyelectrolyte complexes with the coronae via electrostatic interactions.

Complexes of oppositely charged polyelectrolytes[9−16] are known to possess a unique peculiarity: the opposite tendencies, such as intermolecular attraction and solubility of the complexes, can have a common electrostatic origin.[17−19] It is believed that the short-range attraction of oppositely charged units is mediated by thermodynamic fluctuations of the charges[20,21] (relatively weak electrostatic interactions similarly with those of the Debye−Hückel plasma) or by strong multipole (dipole, quadrupole, etc.) interactions of paired oppositely charged groups.[22,23] On the other hand, solubility of the complexes can be attributed to the existence of the long-range electrostatic forces due to the local violation of electric neutrality of the system.[17−19] The most efficient tool controlling solubility of the complexes is a relative fraction of polycations and polyanions in the solutions.[24−26] In asymmetric solutions (the total bare charges of polycations and polyanions are not equal to each other), very stable under-[15,16,24,25] or overcharged[24,25,27−32] complexes are formed. On the contrary, in the symmetric solutions short-range attraction between charged groups prevails over long-range repulsion and complexes usually precipitate.[24,25,33] Therefore, if water-soluble micelles having a charged corona are mixed with oppositely charged polyelectrolytes in stoichiometric ratio, the obtained complexes have to precipitate forming dense structured phase with stimuli (pH, salt, temperature) responsive morphology.

In the present paper, we develop a theory predicting various microstructures in the dense phase formed by precipitation of diblock copolymers with hydrophobic and charged blocks via stoichiometric complexation with an oppositely charged linear polyelectrolyte.

2. Model

Let us consider a solution of an AB diblock copolymer with a neutral, moderately insoluble B block and a charged A block which is fully neutralized via complexation with oppositely charged linear chain of C type, Figure 1. We suppose that both the diblock and the linear chain are flexible and consist of identical statistical segments, each of the length a and of the excluded volume $v \approx a^3$; N_A, N_B, and N_C are the numbers of the segments in the A, B, and C species, respectively. The oppositely charged A block and the C chain are structurally equivalent: they have equal numbers of the segments, $N_A = N_C$, and equal fractions of charged units, $\varphi_A = \varphi_C \equiv \varphi < 1$, so that the A−C complex is stoichiometric. Taking into account insolubility of A−C complexes due to short-range fluctuations induced electrostatic attraction, macromolecules precipitate, forming dense phase. Let us assume that the B blocks are strongly incompatible with the A and/or C species and microdomains of a well-defined shape with narrow interfaces (the strong segregation regime) are formed: globular domains enriched by B or A + C monomer units contain some fraction of the solvent. A competition of the interfacial interactions with the entropic elasticity of the blocks

*To whom correspondence should be addressed. E-mail: igor@polly.phys.msu.ru.

 Published on Web 02/15/2010

Figure 1. Sketch of diblock copolymer comprising nonionic and ionic blocks. Oppositely charged linear chain forms complex with the ionic block.

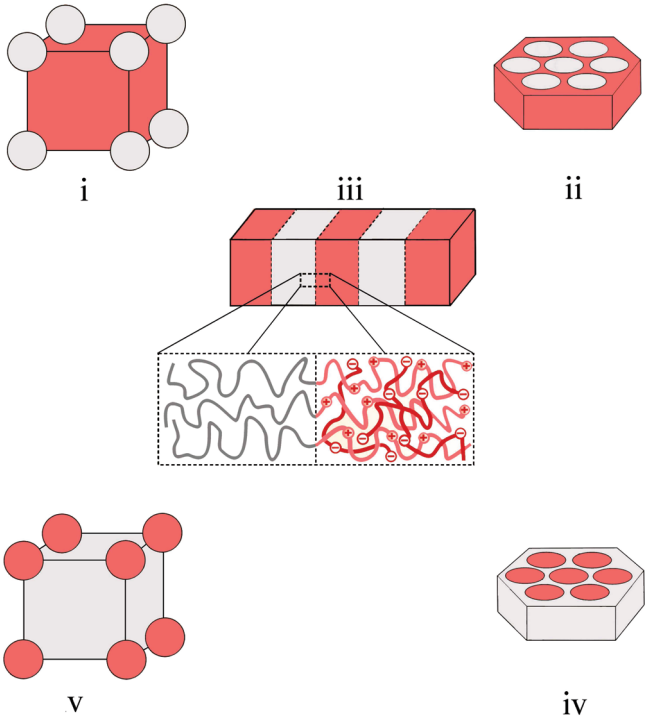

Figure 2. Bcc-packed spherical micelles with (i) nonionic (B) and (v) ionic (A + C) cores, hexagonally packed cylindrical micelles with (ii) nonionic and (iv) ionic cores, and (iii) lamellar structure.

can lead to the formation of various microstructures. The type of the structure depends on the relative lengths of the blocks, $f = N_B/(N_A + N_B)$, on the fraction of charged groups, φ, and on the interaction parameters. For the described system, we will examine conditions for the stability of bcc-packed spherical micelles with (i) nonionic (B) and (ii) ionic (A + C) cores, hexagonally packed cylindrical micelles with (iii) nonionic and (iv) ionic cores, and (v) lamellar structure, Figure 2.

2.1. Spherical Micelles with Nonionic Core. It is assumed that the core of the micelle formed by the B blocks contains some fraction of the solvent. Such regime is realized if the solvent is moderately poor, i.e., one deals with temperatures which are relatively close to the Θ-temperature. Similar to single chain globules,[34] we expect that the core of the micelle has homogeneous density and the space-filing condition reads

$$\frac{4\pi}{3}R^3\phi = QN_Bv \tag{1}$$

where R and Q are the radius of the core and the aggregation number of the micelle, respectively; ϕ is the polymer volume fraction in the core. Complexed A blocks and C chains form a matrix in which the B spheres are ordered with the symmetry of the bcc lattice. Within the spherical approximation for the Wigner−Seitz cell, the A blocks and the C chains in each micelle occupy a spherical layer of the outer radius R_0 (the radius of the cell). Taking into account attractive interactions between the charged groups and restricting our analysis by the Θ-regime for neutral species of both the A block and the C chain, one can expect formation of weakly fluctuating globular state of the corona with homogeneous polymer density. Then the space-filling condition has a simple form:

$$\frac{4\pi}{3}({R_0}^3 - R^3)\psi = 2QN_Av \tag{2}$$

where ψ is the polymer (polycations + polyanions) volume fraction.

The total free energy of the spherical micelle per molecule can be written as a sum of five terms:

$$F^n_{sph} = F^A_{el} + F^B_{el} + F^{core}_{vol} + F^{corona}_{vol} + F_{int} \tag{3}$$

The first two terms are the free energies of radial stretching of the A and B blocks. In contrast to the A blocks, the neutralizing C chains are not stretched because they are not grafted to the AB interface and local neutrality of the corona can be achieved via collective effect: each non-stretched C chain compensates charges located on different A blocks. Spatially inhomogeneous stretching of the A blocks can be calculated in a standard way (k_BT being the thermal energy):

$$\frac{F^A_{el}}{k_BT} = \frac{3}{2a^2}\int_R^{R_0} \mathrm{d}r\, E(r) \tag{4}$$

where the local stretching of the block $E(r) = \mathrm{d}r/\mathrm{d}n$ (derivative of the radial coordinate, r, $R < r < R_0$, over the number of segments, n, $0 < n < N_A$) depends on the coordinate. This dependence can be derived from the space-filling condition of A monomer units: a thin spherical layer of the thickness $\mathrm{d}r$ contains $Q\,\mathrm{d}n$ A segments so that $4\pi r^2\,\mathrm{d}r\,\psi/2 = Q\,\mathrm{d}n\,v$ (the volume fraction of A units is equal to $\psi/2$). Therefore,

$$\frac{F^A_{el}}{k_BT} = \frac{3}{2a^2}\int_R^{R_0}\mathrm{d}r\,\frac{Qa^3}{2\pi\psi r^2} = \frac{R^2}{a^2N_B}\frac{\phi}{\psi}\left(1 - \left[1 + \frac{2N_A\phi}{N_B\psi}\right]^{-1/3}\right) \tag{5}$$

where the space filling conditions, eqs 1 and 2, are used.

By analogy with the strong segregation approximation for flexible diblock copolymers in the melt,[35] the free energy of stretching of the B blocks takes the form:

$$\frac{F^B_{el}}{k_BT} = \frac{3\pi^2}{80}\frac{R^2}{N_Ba^2} \tag{6}$$

The third term in eq 3 is the volume free energy of the core, which describes interactions of monomer units in poor solvent. Assuming relatively small polymer volume fraction in the core, $\phi \ll 1$, one can use the virial approximation[34]

$$\frac{F^{core}_{vol}}{k_BT} = N_B(B\phi + C\phi^2 + \ldots) \tag{7}$$

where B and C are dimensionless second and third virial coefficients. In poor solvent, $B < 0$ and $C > 0$.

The fourth term in eq 3 is the volume contribution to the free energy of the complexed blocks and linear chains

$$\frac{F_{vol}^{corona}}{k_B T} = 2N_A\left[C\psi^2 + \left(\frac{64}{3\pi\psi}\right)^{1/4}\left(\frac{l_B\varphi^2}{a}\right)^{3/4}\right] \quad (8)$$

The formation of the complex can not be described within the mean-field approximation: the Coulomb term is equal to zero at this level. One has to include at least fluctuations around the electroneutral state to describe the complexation. The simplest way to do it is to use the random phase approximation (RPA) formalism.[19−21] The first term in eq 8 describes hard core repulsive interactions of monomer units in the Θ-solvent. The second term is the RPA correction to the mean-field free energy.[19−21] It is responsible for the fluctuations induced attraction of charged units. The Bjerrum length $l_B = e^2/(\varepsilon k_B T)$ quantifies the strength of the electrostatic interactions. For monovalent ions (e is an elementary charge) in water (dielectric constant $\varepsilon \approx 80$), $l_B \approx$ a and oppositely charged ions do not form pairs. The latter can be stable only at higher values of l_B, $l_B > 5a$,[22] when the energy of electrostatic attraction dominates over the thermal energy. This regime is realized in the case of multivalent ions or low dielectric constant.

Finally, the last term in eq 3 is the energy of the core−corona interface. It is responsible for minimization of the number of unfavorable contacts of monomer units of different species with the solvent and with each other:

$$\frac{F_{int}}{k_B T} = \frac{4\pi R^2\gamma}{k_B TQ} = \frac{3\overline{\gamma}N_B a}{R\phi} \quad (9)$$

where γ is the surface tension coefficient. Relying on small polymer concentrations in the core and the corona, one can expect that the main contributions to γ come from the A + C polymer/solvent and the B polymer/solvent interactions whereas interactions of the B and the A + C polymers are negligible. Then γ is a sum of two terms, $\gamma = \gamma_1 + \gamma_2$, calculated in the Appendix:

$$\overline{\gamma} \equiv \frac{\gamma a^2}{k_B T} = \frac{0.11}{C^{7/18}}\left(\frac{l_B\varphi^2}{a}\right)^{2/3} + \frac{\sqrt{6}B^2}{48C^{3/2}} \quad (10)$$

Collecting all contributions together, one gets the following expression for the free energy of the spherical structure:

$$\frac{F_{sph}^n}{k_B T} = \frac{R^2}{a^2 N_B}\left\{\frac{3\pi^2}{80} + \frac{\phi}{\psi}\left(1 - \left[1 + \frac{2N_A\phi}{N_B\psi}\right]^{-1/3}\right)\right\} + \frac{3\overline{\gamma}N_B a}{R\phi} + N_B(B\phi + C\phi^2) + 2N_A\left[C\psi^2 + \left(\frac{64}{3\pi\psi}\right)^{1/4}\left(\frac{l_B\varphi^2}{a}\right)^{3/4}\right] \quad (11)$$

The equilibrium value of F_{sph}^n is calculated via minimization over parameters R, ψ and ϕ what can partially be done analytically (over R):

$$\frac{F_{sph}^n}{k_B T} = \frac{3}{2}\left(\frac{18N_B\overline{\gamma}^2}{\phi^2}\left\{\frac{3\pi^2}{80} + \frac{\phi}{\psi}\left(1 - \left[1 + \frac{2N_A\phi}{N_B\psi}\right]^{-1/3}\right)\right\}\right)^{1/3} + N_B(B\phi + C\phi^2) + 2N_A\left[C\psi^2 + \left(\frac{64}{3\pi\psi}\right)^{1/4}\left(\frac{l_B\varphi^2}{a}\right)^{3/4}\right] \quad (12)$$

$$R = a\left(\frac{3\overline{\gamma}N_B{}^2}{2\phi\left\{\frac{3\pi^2}{80} + \frac{\phi}{\psi}\left(1 - \left[1 + \frac{2N_A\phi}{N_B\psi}\right]^{-1/3}\right)\right\}}\right)^{1/3}$$

and numerically (over ψ and ϕ).

2.2. Spherical Micelles with Ionic Core. The total free energy of the spherical micelle with ionic core has the same structure as F_{sph}^n (eq 3) and calculations of each contribution to the total free energy are straightforward. The free energy as a function of the polymer volume fractions ψ and ϕ takes the form:

$$\frac{F_{sph}^i}{k_B T} = \frac{3}{2}\left(\frac{72N_A\overline{\gamma}^2}{\psi^2}\left\{\frac{3\pi^2}{80} + \frac{\psi}{4\phi}\left(1 - \left[1 + \frac{N_B\psi}{2N_A\phi}\right]^{-1/3}\right)\right\}\right)^{1/3} + N_B(B\phi + C\phi^2) + 2N_A\left[C\psi^2 + \left(\frac{64}{3\pi\psi}\right)^{1/4}\left(\frac{l_B\varphi^2}{a}\right)^{3/4}\right] \quad (13)$$

$$R = a\left(\frac{3\overline{\gamma}N_A{}^2}{\psi\left\{\frac{3\pi^2}{80} + \frac{\psi}{4\phi}\left(1 - \left[1 + \frac{N_B\psi}{2N_A\phi}\right]^{-1/3}\right)\right\}}\right)^{1/3}$$

and the space-filling conditions

$$\frac{4\pi}{3}({R_0}^3 - R^3)\phi = QN_B v$$

$$\frac{4\pi}{3}R^3\psi = 2QN_A v \quad (14)$$

determine the aggregation number, Q, and the radius of the Wigner−Seitz sell (semidistance between the micelles), R_0.

2.3. Cylindrical Micelles with Nonionic Core. The elastic free energy of homogeneously "swollen" core (the core containing a fraction of poor solvent) can be approximated by that derived for the case of a dense micelle[35]:

$$\frac{F_{el}^B}{k_B T} = \frac{\pi^2}{16}\frac{R^2}{N_B a^2} \quad (15)$$

and the local stretching of the A blocks in the corona, $E(r) = dr/dn$, is calculated from the space-filling condition for thin cylindrical layer, $2\pi r\ dr\ \psi/2 = q\ dn\ v$, $E(r) = qv/(\pi\psi r)$, where $q = Q/L$ is the aggregation number per unit length of the cylinder, whereas the total aggregation number, Q, and the length of the cylinder, L, are infinite, $L, Q = \infty$. The elastic free energy of the A block in the corona reads

$$\frac{F_{el}^{A}}{k_{\mathrm{B}}T} = \frac{3}{2a^2}\int_{R}^{R_0} dr\ E(r) = \frac{R^2}{N_B a^2}\frac{3\phi}{4\psi}\ln\left(1+\frac{2N_{\mathrm{A}}\phi}{N_B\psi}\right) \quad (16)$$

where the space-filling conditions

$$\pi R^2\phi = N_B q v$$

$$\pi(R_0{}^2 - R^2)\psi = 2N_{\mathrm{A}} q v \quad (17)$$

are used. Taking the surface energy per chain in the form $2\bar{\gamma}N_B a/(R\phi)$, one gets the total free energy (see eq 3)

$$\frac{F_{cyl}^{n}}{k_{\mathrm{B}}T} = \frac{3}{2}\left(\frac{8N_B\bar{\gamma}^2}{\phi^2}\left\{\frac{\pi^2}{16}+\frac{3\phi}{4\psi}\ln\left(1+\frac{2N_{\mathrm{A}}\phi}{N_B\psi}\right)\right\}\right)^{1/3} + N_B(B\phi + C\phi^2) + 2N_{\mathrm{A}}\left[C\psi^2 + \left(\frac{64}{3\pi\psi}\right)^{1/4}\left(\frac{l_B\varphi^2}{a}\right)^{3/4}\right] \quad (18)$$

$$R = a\left(\frac{\bar{\gamma}N_B{}^2}{\phi\left\{\frac{\pi^2}{16}+\frac{3\phi}{4\psi}\ln\left(1+\frac{2N_{\mathrm{A}}\phi}{N_B\psi}\right)\right\}}\right)^{1/3}$$

after minimization over R.

2.4. Cylindrical Micelles with Ionic Core. The total free energy of the cylindrical micelle with the ionic (A + C) core is derived in a similar way as for the case of the micelles with nonionic cylindrical core

$$\frac{F_{cyl}^{i}}{k_{\mathrm{B}}T} = \frac{3}{2}\left(\frac{32N_{\mathrm{A}}\bar{\gamma}^2}{\psi^2}\left\{\frac{\pi^2}{16}+\frac{3\psi}{16\phi}\ln\left(1+\frac{N_B\psi}{2N_{\mathrm{A}}\phi}\right)\right\}\right)^{1/3} + N_B(B\phi + C\phi^2) + 2N_{\mathrm{A}}\left[C\psi^2 + \left(\frac{64}{3\pi\psi}\right)^{1/4}\left(\frac{l_B\varphi^2}{a}\right)^{3/4}\right] \quad (19)$$

$$R = a\left(\frac{2\bar{\gamma}N_A{}^2}{\psi\left\{\frac{\pi^2}{16}+\frac{3\psi}{16\phi}\ln\left(1+\frac{N_B\psi}{2N_{\mathrm{A}}\phi}\right)\right\}}\right)^{1/3}$$

and the space-filling conditions take the form:

$$\pi(R_0^2 - R^2)\phi = qN_B v$$

$$\pi R^2\psi = 2qN_{\mathrm{A}} v \quad (20)$$

2.5. Lamellar Structure. The elastic free energies of the A and B blocks in lamellae have similar form[35]

$$\frac{F_{el}^{A}+F_{el}^{B}}{k_{\mathrm{B}}T} = \frac{\pi^2}{8}\frac{R^2}{N_{\mathrm{A}}a^2} + \frac{\pi^2}{8}\frac{(R_0-R)^2}{N_B a^2} = \frac{\pi^2}{8}\frac{R^2}{N_{\mathrm{A}}a^2}\left(1+\frac{N_B\psi^2}{4N_{\mathrm{A}}\phi^2}\right) \quad (21)$$

where semithicknesses of the ionic layer, R, and nonionic layer, $R_0 - R$, are related through the space-filling conditions

$$2R\psi = 2qN_{\mathrm{A}} v$$

$$2(R_0 - R)\phi = qN_B v \quad (22)$$

Here q is the aggregation number per unit area of the lamella. The interfacial energy per molecule is $2\bar{\gamma}N_A a/(R\psi)$ and minimization of the total free energy, eq 3, over R results in the following expression:

$$\frac{F_{lam}}{k_{\mathrm{B}}T} = \frac{3}{2}\left(\frac{N_{\mathrm{A}}\pi^2\bar{\gamma}^2}{\psi^2}\left\{1+\frac{N_B\psi^2}{4N_{\mathrm{A}}\phi^2}\right\}\right)^{1/3} + N_B(B\phi + C\phi^2) + 2N_{\mathrm{A}}\left[C\psi^2 + \left(\frac{64}{3\pi\psi}\right)^{1/4}\left(\frac{l_B\varphi^2}{a}\right)^{3/4}\right] \quad (23)$$

$$R = a\left(\frac{8\bar{\gamma}N_A{}^2}{\pi^2\psi\left\{1+\frac{N_B\psi^2}{4N_{\mathrm{A}}\phi^2}\right\}}\right)^{1/3}$$

3. Results and Discussion

The phase diagrams of the AB diblock copolymers complexed with the linear C chains in stoichiometric ratio are constructed via numerical solution of the equations $F_{sph}^{n} = F_{cyl}^{n}$, $F_{cyl}^{n} = F_{lam}$, $F_{lam} = F_{cyl}^{i}$, and $F_{cyl}^{i} = F_{sph}^{i}$ after minimization of the corresponding expressions, eqs 12, 13, 18, 19, 23 over the parameters ϕ and ψ. The parameters controlling phase behavior are f, φ, B, C, l_B, and N. In all our calculations we fix the values of the third virial coefficient, $C = 1$, and of the Bjerrum length, $l_B = a$. The latter equality corresponds to aqueous solutions where oppositely charged monovalent ions do not form pairs (relatively weak electrostatic interactions). The absolute value of the second virial coefficient has to be much smaller than unity, $|B| \ll 1$, to justify the virial approximation. However, qualitatively correct result can be obtained even at $|B| \sim 1$.

The $f - \varphi$ phase diagrams in Figure 3 are plotted at $B = -0.1$ and different values of the number of segments in the diblock, N: 100 (a), and 1000 (b), whereas the diagrams in Figure 4 are plotted at a smaller value of the second virial coefficient, $B = -0.5$. Similar to the conventional phase diagram of the melt of diblock copolymers, alteration of microphases with increasing relative length of the nonionic block, $f = N_B/(N_A + N_B)$, looks like: nonionic (B) spheres−nonionic (B) cylinders−lamellae−ionic (A) cylinders−ionic (A) spheres, Figures 3 and 4. However, transition values of f depend on the fraction of charged groups in the ionic block: the higher is the fraction, the smaller are the

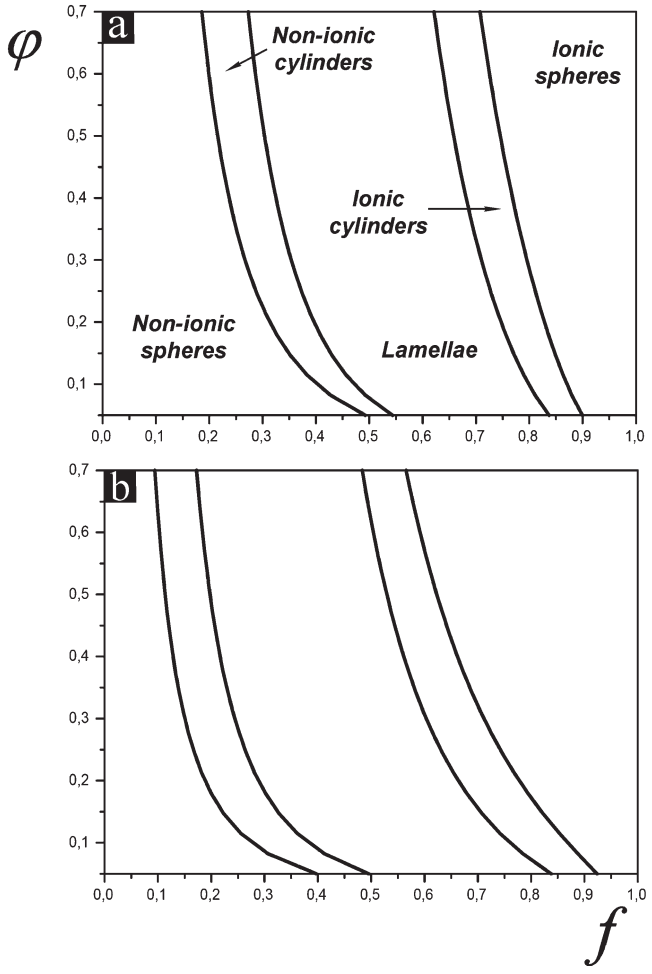

Figure 3. $f-\varphi$ phase diagrams at different values of the number of segments in the copolymer: $N = 100$ (a) and 1000 (b). $B = -0.1$. Relative positions of different phases in part b are the same as in part a.

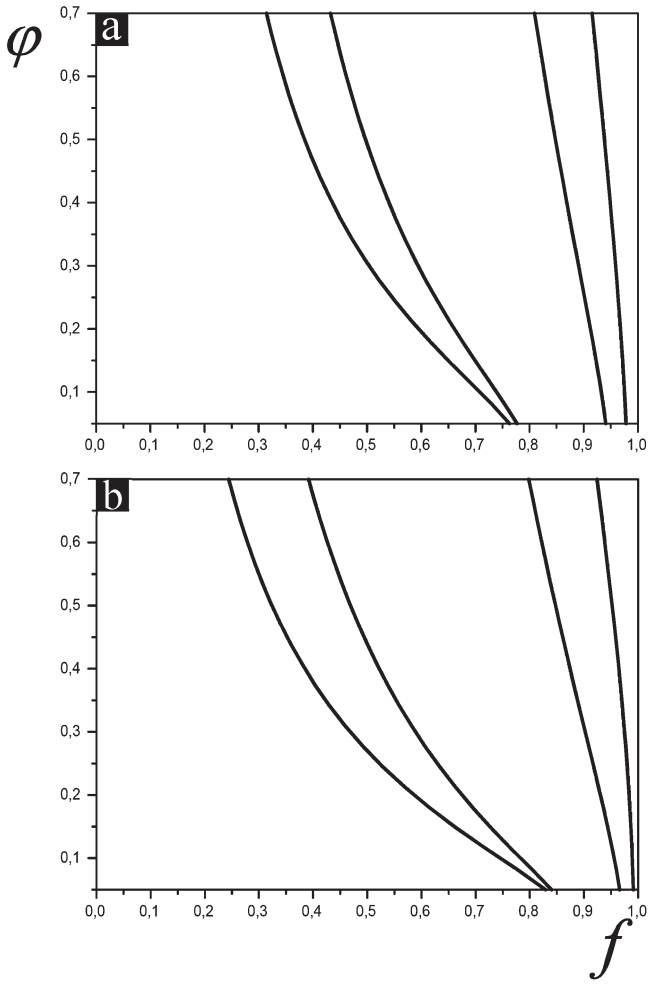

Figure 4. $f-\varphi$ phase diagrams at different values of the number of segments in the copolymer: $N = 100$ (a) and 1000 (b). $B = -0.5$. Relative positions of different phases in Figure 4 are the same as in Figure 3a.

values of f. This effect has a clear physical meaning. Stronger charged polyelectrolyte blocks and linear chains form more compact (denser) complexes because of enhanced electrostatic interactions[19] resulting in a smaller radial stretching of the A blocks. Since the microstructure type depends on the relative stretching of the A and B blocks, transitions between various microphases shift to smaller N_B (f) with an increase of φ (shrinkage of A blocks). In other words, variation of the fraction of charged groups (pH-responsive weak polyelectrolytes) controls stretching of the ionic block and can induce a morphology change, this phenomenon is clearly seen in Figures 3 and 4. For example, an asymmetric copolymer (with a longer hydrophobic block, $f \approx 0.6-0.75$, Figure 4) reveals the following transitions with the increase of φ: nonionic spheres → nonionic cylinders → lamellae.

Effect of the second virial coefficient on the phase diagrams is demonstrated in Figures 3 and 4. Worsening of the solvent quality for the B blocks (decrease of B) causes a shrinkage of the B blocks, i.e., compaction of the hydrophobic domains. As a result, all boundaries between microphases shift toward higher values of f with the increase of $|B|$. Therefore, inducing transition from nonionic spheres to cylinders with shrunken B block, one has to deal with shorter A blocks, i.e., higher f in comparison with nonshrunken B block. The slope of the boundaries in $B-f$ diagrams, Figure 5, enables us to conclude that variation of the solvent quality for hydrophobic blocks can also induce structural transitions.

One can analyze the effect of the overall length of the diblock on phase behavior comparing the a and b diagrams in Figures 3 and 4. Longer molecules exhibit all transitions at smaller values of f as an onset of the coupling of the interfacial (elastic) and volume contributions to the free energies of the corresponding structures via parameters ϕ and ψ. Minimization of eqs 12, 13, 18, 19, and 23 gives weak dependence of ϕ and ψ on N: $\psi, \phi \sim const + \overline{const}/N^{2/3}$, $N \gg 1$, if we use the perturbation theory assuming that the volume contributions ($\sim N_A$ and N_B) are dominant. Thus, the blocks' stretching weakly depends on the overall length. In the limit of infinitely long molecules, $N \to \infty$, and $N_A \sim N_B$ (the composition f tend to neither 0 nor 1), the polymer volume fractions in ionic and nonionic domains do not depend on the length of the molecules and can be calculated via minimization of the volume contributions, eqs 12, 13, 18, 19, and 23:

$$\phi = -\frac{B}{2C}$$

$$\psi = \frac{(l_B/a)^{1/3}\varphi^{2/3}}{(12\pi)^{1/9}(2C)^{4/9}} \tag{24}$$

These values are the same for all microstructures and correspond to the polymer volume fraction ϕ of single globule in a poor solvent[34] and to the polymer volume fraction ψ of complexed linear chains.[19] The latter result, $\psi \sim (l_B/a)^{1/3}\varphi^{2/3}$, can also be derived using the scaling approach, where the complex of

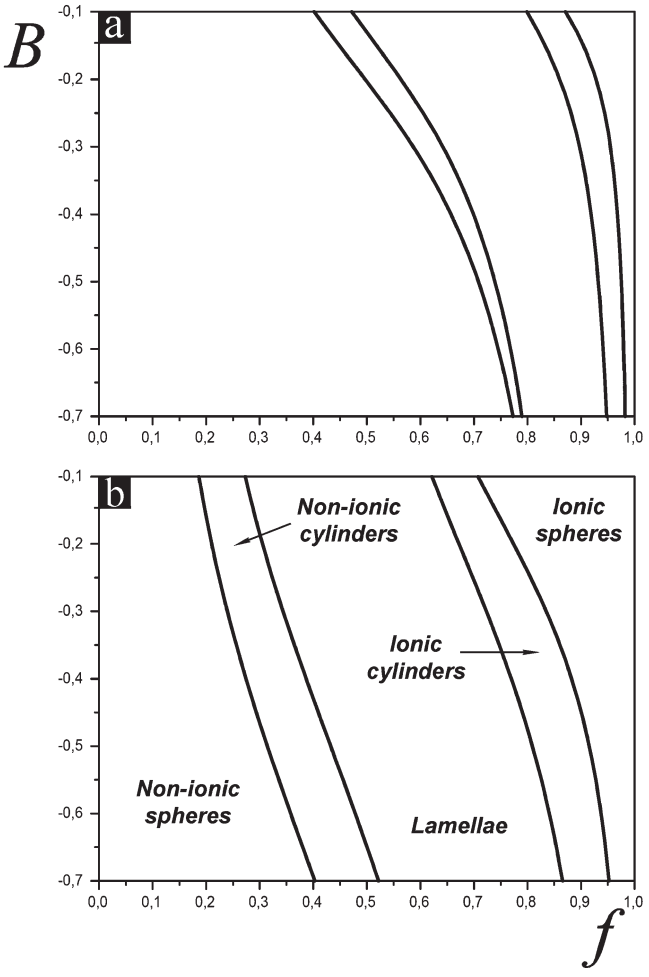

Figure 5. $f-B$ phase diagrams at different values of the fraction of charged units in the ionic block: $\varphi = 0.1$ (a) and 0.7 (b). $N = 100$. Relative positions of different phases in part a are the same as in part b.

oppositely charged polyelectrolytes is described in terms of electrostatic attraction blobs.[18]

In the limit $N \rightarrow \infty$, the boundaries of stability of various microphases can be calculated analytically. For symmetric copolymer, $N_A = N_B$, the transitions: nonionic spheres → nonionic cylinders → lamellae → ionic cylinders → ionic spheres occur at

$$\frac{\phi}{\psi} = -\frac{(12\pi)^{1/9}B}{(2C)^{5/9}(l_B/a)^{1/3}\varphi^{2/3}} \approx 1.25,\ 0.9,\ 0.28,\ 0.2 \qquad (25)$$

respectively. The $\varphi-B$ phase diagram for symmetric AB copolymer calculated with the use of eq 25 is plotted in Figure 6. The microstructures with ionic spheres and cylinders are stable at small absolute values of the second virial coefficient because only in this case the nonionic blocks can have higher radial stretching than the ionic blocks. It has to be reminded that if both ionic and nonionic domains are even free of the solvent, the A blocks have higher stretching than the B blocks because complexed C chains play a role of a solvent. Therefore, inducing structures with ionic cores, one has to "swell" (elongate) B block higher than the A ones. That is why the areas of stability of the ionic spheres and cylinders are relatively small, Figure 6. Also, Figure 6 demonstrates that variation of the solvent quality (temperature) within a narrow interval allows to observe all possible microstructures if the fraction of charged groups in the ionic block is relatively small (left side of the diagram). In other words, the smaller is the φ, the stronger is the response of the morphology to the temperature.

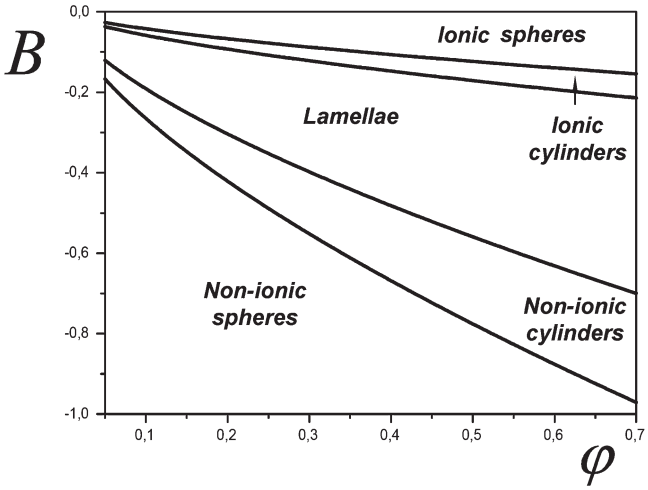

Figure 6. $\varphi-B$ phase diagram of the symmetric copolymer ($f = {}^1/_2$) obtained at $N \rightarrow \infty$.

An obvious restriction on the minimum value of φ is the threshold of complexation. Analysis of the critical point of counterions-free solution of oppositely charged linear chains in Θ-solvent[36] and scaling analysis for diblock polyampholytes in Θ-solvent[18] predict complexation at $\varphi > \varphi_c \sim N^{-3/4}(l_B/a)^{-1/2}$. Thus, φ_c is very small and tends to zero at $N \rightarrow \infty$.

Phase diagram of the system does not depend on the surface tension coefficient $\bar{\gamma}$ at $N \rightarrow \infty$: in equalities of the free energies, $F^n_{sph} = F^n_{cyl}$, $F^n_{cyl} = F_{lam}$, $F_{lam} = F^i_{cyl}$, and $F^i_{cyl} = F^i_{sph}$, eqs 12, 13, 18, 19, and 23, the volume contributions ($\sim N$) are canceled (ψ and ϕ for all structures are done by eq 24) and each nonvolume term ($\sim N^{1/3}$) contains multiplier $\bar{\gamma}^{2/3}$. The only restriction imposed on the value of the surface tension coefficient is that it has to provide the strong segregation condition. The latter means that the surface energy per chain, which is on the order of magnitude of the elastic free energy (minimization over R establishes such interrelation), must be much larger than the energy of translational motion of the molecule. The surface and the elastic free energies are given by first terms in eqs 12, 13, 18, 19, and 23. At the transition point, $\phi/\psi = const\,(B \sim -C^{5/9}(l_B/a)^{1/3}\varphi^{2/3})$, eq 25, and the strong segregation condition takes the form:

$$\frac{N\bar{\gamma}^2}{\phi^2} \gg 1, \quad \text{or} \quad \frac{NB^2}{C} \gg 1 \qquad (26)$$

what is always fulfilled at $1 > |B| \gg N^{-1/2}$. In the diagrams presented, we do not depict spatially homogeneous phases. Such phases are formed if the length of A (or B) block is exponentially small.[35] They occupy very narrow regions in close vicinity to $f = 0$ and 1.

4. Conclusion

We have developed a strong segregation theory of microphase separation in solution of AB block copolymers and linear chains. One of the blocks of the copolymer (A) is charged and neutral block (B) is moderately insoluble (the globular domains formed by the B blocks can contain some fraction of the solvent). Oppositely charged linear chains (C) form stoichiometric complexes with the A blocks. In semidilute solution, complexed diblock copolymers and linear chains precipitate due to attractive fluctuations induced electrostatic interactions. Incompatibility of B with A + C species results in structuring of the precipitant. We predicted thermodynamic stability of bcc-packed spherical micelles with (i) nonionic (B) and (ii) ionic (A + C) cores, hexagonally packed cylindrical micelles with (iii) nonionic and

(iv) ionic cores, and (v) lamellar structure. Phase diagrams of microphase separation are constructed. In the case of weak polyelectrolytes, morphological transitions can be induced by variation of both pH and solvent quality.

Optimum conditions for the stability of the mentioned morphologies can be summarized as follows.

1 **Nonionic Spheres:** short hydrophobic (B) block; relatively small fraction of charged groups in the A block and the C chain; high insolubility of the B block.
2 **Nonionic Cylinders:** short hydrophobic block (but longer than in case 1) whose length is related to the solvent quality: the poorer the solvent, the longer the B block; relatively high fraction of charged groups.
3 **Lamellae:** symmetric and weakly asymmetric copolymer; high fraction of charged groups.
4 **Ionic Cylinders:** relatively short charged block whose length is related to the solvent quality: the poorer the solvent, the shorter the A block.
5 **Ionic Spheres:** short charged block; high fraction of charged units; moderate insolubility of the B block.

Acknowledgment. The financial support of the Russian Foundation for Basic Research, the Deutsche Forschungsgemeinschaft within SFB 569, the Federal Agency for Science and Innovation (Russian Federation), and the Dynasty Foundation (Russian Federation) is gratefully acknowledged.

Appendix

Within our approach, γ_1 is equivalent to the surface tension coefficient of the interface between complexed linear chains and pure Θ-solvent (the grafting of the A chains to the interface is negligible). For the latter system, γ_1 is calculated via minimization of one-dimensional functional:

$$\frac{\gamma_1}{k_B T} = \int_{-\infty}^{+\infty} \frac{dx}{v}\left[\frac{a^2(\psi'(x))^2}{24\ \ \psi(x)} + C\psi(x)^3 + \left(\frac{64}{3\pi}\right)^{1/4}\left(\frac{\psi(x) l_B \varphi^2}{a}\right)^{3/4} + \mu\psi(x)\right] \quad (27)$$

over the polymer volume fraction, $\psi(x)$, that depends on the normal coordinate x in vicinity of the interface ($x = 0$). It is assumed that $\psi(x)$ monotonously grows from 0 in pure solvent (at $x = -\infty$) to some constant value ψ_0 inside the complex far from the interface (at $x = +\infty$). Therefore, obvious boundary conditions imposed on $\psi(x)$ are $\psi(-\infty) = 0$, $\psi(+\infty) = \psi_0$, and all derivatives (first, second, etc.) of $\psi(x)$ over x at $x = \pm\infty$ are equal to zero, $\psi'(\pm\infty) = \psi''(\pm\infty) = ... = 0$ ($\psi(x)$ is a step-like function in the shape). The first term of eq 27 is the conventional gradient term[34] that describes entropic losses of the chains because of inhomogeneous density near the interface. The next two terms are the coordinate-dependent contributions to the volume free energy, eq 8, and the last term is introduced to take into account normalization of $\psi(x)$; μ is the Lagrange multiplier.

Minimization of the functional 27 can be done in a standard way using substitution $\psi(x) = y(x)^2$:

$$-\frac{a^2}{3}y'' + 6Cy^5 + \left(\frac{64}{3\pi}\right)^{1/4}\left(\frac{l_B\varphi^2}{a}\right)^{3/4}\frac{3}{2}y^{1/2} + 2\mu y = 0 \quad (28)$$

where the boundary conditions are

$$y(-\infty) = 0, \quad y(+\infty) = y_0 = \sqrt{\psi_0}$$

$$y'(\pm\infty) = y''(\pm\infty) = ... = 0 \quad (29)$$

Equation 28 can be integrated after multiplying by y':

$$-\frac{a^2}{6}(y')^2 + Cy^6 + \left(\frac{64}{3\pi}\right)^{1/4}\left(\frac{l_B\varphi^2}{a}\right)^{3/4} y^{3/2} + \mu y^2 = 0 \quad (30)$$

where the constant of integration is set equal to zero due to the boundary conditions at $x = -\infty$. Applying the boundary conditions at $x = +\infty$ to eqs 28 and 30, we get

$$y_0 = \left(\frac{1}{(3\pi)^{1/4}C}\left(\frac{l_B\varphi^2}{4a}\right)^{3/4}\right)^{2/9}, \quad \mu = -9Cy_0{}^4 \quad (31)$$

Using eq 30, one can present the surface tension coefficient as follows:

$$\frac{\gamma_1}{k_B T} = \int_{-\infty}^{+\infty}\frac{dx a^2 (y')^2}{v\ \ 3} = \frac{a^2}{3v}\int_0^{y_0} dy\, y'$$
$$= \frac{a\sqrt{6}}{3v}\int_0^{y_0} dy \sqrt{Cy^6 + \left(\frac{64}{3\pi}\right)^{1/4}\left(\frac{l_B\varphi^2}{a}\right)^{3/4} y^{3/2} + \mu y^2}$$
$$= \frac{a\sqrt{6C}y_0^4}{3v}\int_0^1 dt\ \sqrt{t^6 + 8t^{3/2} - 9t^2} \approx \frac{0.11}{C^{7/18}a^2}\left(\frac{l_B\varphi^2}{a}\right)^{2/3} \quad (32)$$

Similar calculations are valid for derivation of the second contribution, γ_2, coming from interactions of B polymer with the solvent. In this case, the third term in eq 27 has to be substituted by that responsible for pairwise attraction of monomer units in the neutral globule, $B\psi^2(x)$ (see eq 7). The result can be written as[37]

$$\frac{\gamma_2}{k_B T} = \frac{\sqrt{6}B^2}{48C^{3/2}a^2} \quad (33)$$

References and Notes

(1) Khokhlov, A. R.; Nyrkova, I. A. *Macromolecules* **1992**, *25*, 1493.
(2) Vasilevskaya, V. V.; Potemkin, I. I.; Khokhlov, A. R. *Langmuir* **1999**, *15*, 7918.
(3) Zhang, L.; Eisenberg, A. *Science* **1995**, *268*, 1728.
(4) Soo, P. L.; Eisenberg, A. *J. Polym. Sci., Part B* **2004**, *42*, 923.
(5) Marko, J. F.; Rabin, Y. *Macromolecules* **1992**, *25*, 1503.
(6) Shusharina, N. P.; Nyrkova, I. A.; Khokhlov, A. R. *Macromolecules* **1996**, *29*, 3167.
(7) Borisov, O. V.; Zhulina, E. B. *Macromolecules* **2002**, *35*, 4472.
(8) Borisov, O. V.; Zhulina, E. B. *Langmuir* **2005**, *21*, 3229.
(9) Bakeev, K. N.; Izumrudov, V. A.; Kuchanov, S. I.; Zezin, A. B.; Kabanov, V. A. *Macromolecules* **1992**, *25*, 4249.
(10) Kabanov, A. V.; Bronich, T. K.; Kabanov, V. A.; Yu, K.; Eisenberg, A. *Macromolecules* **1996**, *29*, 6797.
(11) Dautzenberg, H.; Hartmann, J.; Grunewald, S.; Brand, F. *Ber. Bunsen-Ges. Phys. Chem.* **1996**, *100*, 1024.
(12) Pogodina, N. V.; Tsvetkov, N. V. *Macromolecules* **1997**, *30*, 4897.
(13) Dautzenberg, H. *Macromolecules* **1997**, *30*, 7810.
(14) Gohy, J.-F.; Varshney, S. K.; Jerome, R. *Macromolecules* **2001**, *34*, 3361.

(15) Kramarenko, E. Yu.; Khokhlov, A. R.; Reineker, P. *J. Chem. Phys*. **2003**, *119*, 4945.
(16) Kramarenko, E. Yu.; Khokhlov, A. R.; Reineker, P. *J. Chem. Phys*. **2006**, *125*, 194902.
(17) Castelnovo, M.; Joanny, J.-F. *Macromolecules* **2002**, *35*, 4531.
(18) Shusharina, N. P.; Zhulina, E. B.; Dobrynin, A. V.; Rubinstein, M. *Macromolecules* **2005**, *38*, 8870.
(19) Oskolkov, N. N.; Potemkin, I. I. *Macromolecules* **2007**, *40*, 8423.
(20) Borue, V. Yu.; Erukhimovich, I. Ya. *Macromolecules* **1988**, *21*, 3240.
(21) Borue, V. Yu.; Erukhimovich, I. Ya. *Macromolecules* **1990**, *23*, 3625.
(22) Wang, Z.; Rubinstein, M. *Macromolecules* **2006**, *39*, 5897.
(23) Kramarenko, E.Yu.; Khokhlov, A. R. *Polym. Sci., Ser. A* **2007**, *49*, 1053.
(24) Lysenko, E. A.; Chelushkin, P. S.; Bronich, T. K.; Eisenberg, A.; Kabanov, V. A.; Kabanov, A. V. *J. Phys. Chem. B* **2004**, *108*, 12352.
(25) Chelushkin, P. S.; Lysenko, E. A.; Bronich, T. K.; Eisenberg, A.; Kabanov, V. A.; Kabanov, A. V. *J. Phys. Chem. B* **2007**, *111*, 8419.
(26) Hofs, B.; de Keizer, A.; Cohen Stuart, M. A. *J. Phys. Chem. B* **2007**, *111*, 5621.
(27) Rädler, J. O.; Koltover, I.; Salditt, T.; Safinya, C. R. *Science* **1997**, *275*, 810.
(28) Mateescu, E. M.; Jeppesen, C.; Pincus, P. *Europhys. Lett*. **1999**, *46*, 493.
(29) Park, S. Y.; Bruinsma, R. F.; Gelbart, W. M. *Europhys. Lett*. **1999**, *46*, 454.
(30) Nguyen, T. T.; Grosberg, A. Yu.; Shklovskii, B. I. *Phys. Rev. Lett*. **2000**, *85*, 1568.
(31) Potemkin, I. I. *Europhys. Lett*. **2004**, *68*, 487.
(32) Oskolkov, N. N.; Potemkin, I. I. *Macromolecules* **2006**, *39*, 3648.
(33) Kudlay, A.; de la Cruz, M. O. *J. Chem. Phys*. **2004**, *120*, 404.
(34) Grosberg, A. Yu.; Khokhlov, A. R. *Statistical Physics of Macromolecules*; AIP Press: New York, 1994.
(35) Semenov, A. N. *Sov. Phys. JETP* **1985**, *61*, 733.
(36) Potemkin, I. I.; Palyulin, V. V. To be published.
(37) Lifshitz, I. M.; Grosberg, A. Yu.; Khokhlov, A. R. *Rev. Mod. Phys*. **1978**, *50*, 683.